JOURNAL OF GEOPHYSICAL RESEARCH, VOL. 104, NO. D14, PAGES 16,859–16,877, JULY 27, 1999

Extending aircraft- and tower-based CO_2 flux measurements to a boreal region using a Landsat thematic mapper land cover map

Jing M. Chen, Sylvain G. Leblanc, and Josef Cihlar
Canada Centre for Remote Sensing, Ottawa

Raymond L. Desjardins
Agriculture and Agri-Food Canada, Ottawa

J. Ian MacPherson
Flight Research Laboratory, National Research Council of Canada, Ottawa

Abstract. There has been an increasing need to measure the exchange of CO_2 between the atmosphere and vegetated surfaces for large areas in order to quantify the carbon budget of the terrestrial biosphere. The boreal landscape is heterogeneous owing to different forest cover types and disturbance regimes, and regional quantification of CO_2 flux is difficult without numerous species-specific flux measurements. During the Boreal Ecosystem-Atmosphere Study in 1994 and 1996 the National Research Council of Canada operated a Twin Otter aircraft that measured CO_2, sensible and latent heat fluxes, and other trace gases over boreal forests in Saskatchewan, Canada. A flux-unmixing method was developed to calculate flux densities for eight major cover types from the aircraft-based measurements. Using a coregistered land cover map at 30-m resolution derived from Landsat thematic mapper data, the contribution of each cover type to the CO_2 flux measured by the aircraft was estimated using a contributing area (footprint) function according to the wind direction, the atmospheric stability, the horizontal distance of each pixel from the aircraft, and aircraft height. The unmixing method uses a linear inversion method with the footprint-weighted cover type fractions as the set coefficients for each segment of a flight line. In the inversion, various constraint strategies were used to confine the inversion results to minimize the effect of various sampling errors. It is shown that (1) mathematical constraint is critically important in the inversion, (2) a simple constraint toward the mean flux values is effective in producing reasonable inversion results, and (3) the inversion accuracy can be further improved when simultaneous tower measurements in the dominant cover types are used as tight constraints. With such constraints the estimated fluxes from the cover types without tower measurements appear to be reasonable. It is concluded that aircraft measurement adds to our ability to map the regional flux field using remote sensing images because (1) it allows the derivation of flux data for cover types without tower-based measurements and (2) it can be used to infer the representativeness of tower measurements for the measured cover types in the landscape.

1. Introduction

Reliable measurements of carbon exchange between the atmosphere and the land are critical to our understanding of the role of terrestrial ecosystems in the global carbon cycle and the development of models for regional and global applications. Tower-based measurements for a full seasonal cycle have been shown to be useful for quantifying the net carbon exchange of vegetation canopies [*Grace et al*., 1995; *Black et al*., 1997; *Goulden et al*., 1998]. Aircraft-based measurements have been successfully used for many years for measuring regional CO_2 flux [*Desjardins*, 1991; *Desjardins et al*., 1994; *Mitic et al*., 1995; *Ogunjemiyo et al*., 1997]. These two techniques are distinct in their different spatial and temporal characteristics. Tower measurements can be made for long periods and thus provide the temporal integration necessary for determining net carbon exchange for a given period of time (day, month, and year), but the measured results can only represent the small "footprint" area of the tower [*Schuepp et al*., 1990; *Kaharabata et al*., 1997]. An aircraft has the ability to integrate over a long distance along a flight line or an area when flights are made in a grid pattern [*Desjardins et al*., 1995], but the measurements can only be made at discrete times over short periods. For regional quantification of net carbon flux it is therefore desirable to integrate both techniques.

During the Boreal Ecosystem-Atmosphere Study (BOREAS), which took place in Manitoba and Saskatchewan in 1994 and 1996, simultaneous aircraft and tower measurements of CO_2 and other fluxes were made over several types of forest canopies. Maps of the aircraft-measured fluxes were compared with a satellite greenness index, and the spatial distribution patterns were shown within two flight grids [*Ogunjemiyo et al*., 1997]. *Desjardins et al*. [1997] compared Twin Otter aircraft measurements with tower measurements and

Copyright 1999 by the American Geophysical Union.

Paper number 1999JD900129.
0148-0227/99/1999JD900129$09.00

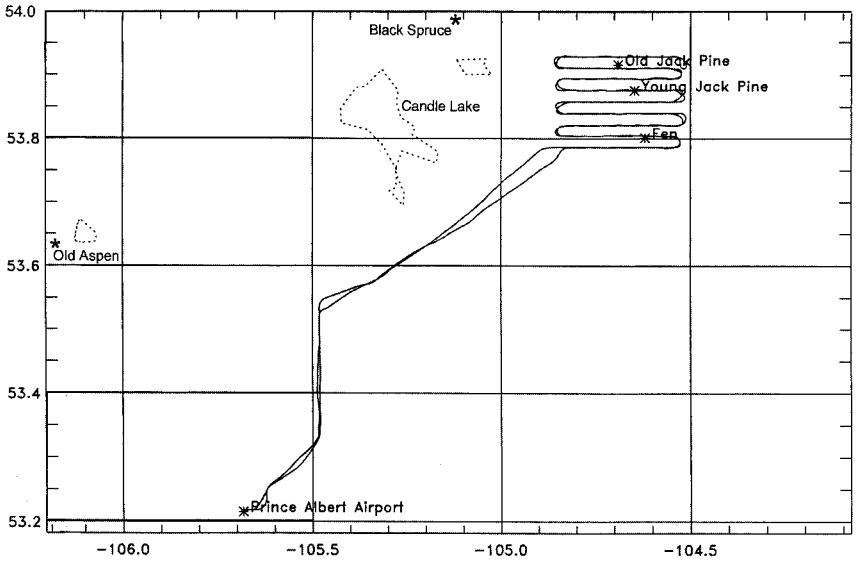

Figure 1. A typical Twin Otter grid flight pattern over the southern BOREAS study area with east-west flight lines.

made the first attempt to estimate the flux for BOREAS southern and northern study areas (SSA and NSA, respectively) using statistics of cover type areas. Two important issues arise from the simple scaling method: (1) the representativeness of tower measurements for the specific cover types in the landscape and (2) the lack of tower measurements for some cover types. Ideally, aircraft measurements can be separated into portions of flux records representing the cover types and provide true averaged values for all cover types involved. However, it is impossible to make such spatial separation explicitly because different cover types are often spatially mixed in a given area and the wind further mixes fluxes to and from adjacent cover types before they are measured at the aircraft position. It is necessary to make such separations by "flux unmixing," i.e., to separate the contributions of different cover types to a flux record measured at a given time and a given location. This is mathematically feasible if a flux record is separated into a number of segments equal to or more than the number of cover types. However, in the execution of the idea the methodology is complicated by the fact that areas of the same cover type at different distances from the aircraft in the wind direction contribute differently to the flux. It therefore becomes imperative to use a distance-weighted cover type fraction for each flux segment according to the wind speed and direction. As we are unaware of similar work done elsewhere, we have developed a mathematical scheme and a model for this purpose. This flux-unmixing method may be an improvement from the empirical "inverse footprint" method of *Schuepp et al*. [1992] used for studies of flux spatial distribution in a grassland.

The overall goal of this paper is to investigate the feasibility of obtaining spatially averaged fluxes for different cover types separately for the purpose of scaling from aircraft measurements to an area. The following methodological issues will be addressed: (1) how to use a remote sensing land cover type map to provide weighted area fractions for different cover types contributing to fluxes measured by an aircraft, (2) how to unmix an aircraft flux record for the different cover types using the weighted area fractions, (3) the methods to constrain unmixing results to minimize the effects of errors in measurements and uncertainties in aircraft footprint calculations due to wind direction variations, and (4) how to use tower-based data, if available, to strengthen the numerical constraint.

2. Data Description

2.1. Aircraft Measurements

During BOREAS field campaigns the National Research Council of Canada (NRC) operated a Twin Otter aircraft [*MacPherson*, 1996; *MacPherson and Bastian*, 1997] over boreal forests in Saskatchewan, Canada. Several instruments were mounted on board measuring its position, the wind speed and direction, the air temperature and humidity, the incident and reflected solar radiation, and the fluxes of carbon dioxide,

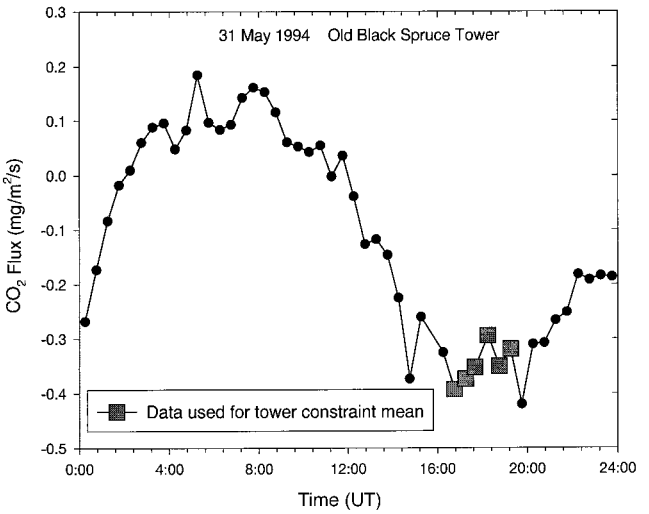

Figure 2. A tower-based CO_2 flux time series for May 31, 1994, over the old black spruce site. The large squares indicate the values during the aircraft grid flight. UT is 5 hours ahead of the local time.

Plate 1. Land cover map of the study area based on a Landsat thematic mapper (TM) image [*Hall et al.*, 1997] with flight lines and footprint areas represented by quadrilaterals associated with each 2-km segment in flight line 1. OJP, old jack pine; YJP, young jack pine.

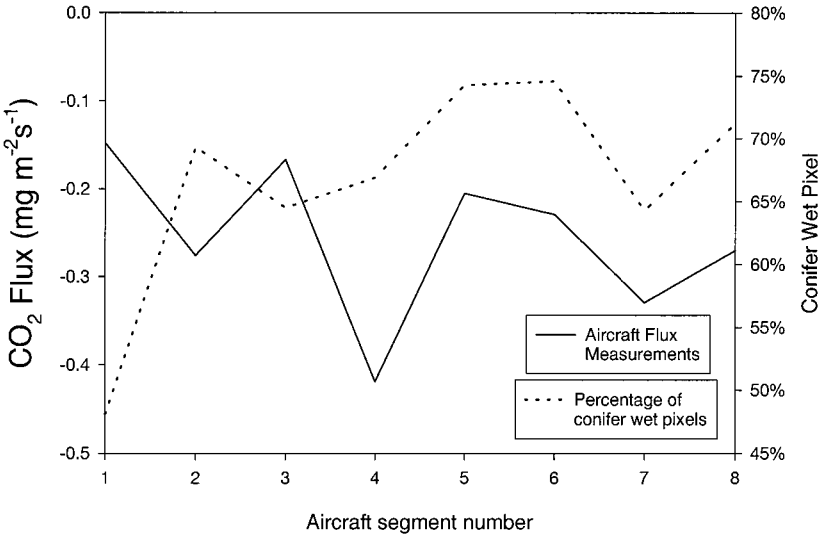

Figure 3. CO_2 flux measured by the aircraft on a single 16-km flight line (the leftmost line on Plate 1) separated into eight segments, May 31, 1994, along with the percentage of pixels for the dominant conifer wet cover type in the footprint area.

sensible and latent heat, and ozone. Two grid patterns in the southern study area (SSA) were flown. One of the patterns is shown in Figure 1. Depending on the wind direction, either east-west or north-south flight lines were chosen to favor cross-wind measurements. The aircraft was flown at an altitude of ~30 m above the tops of the trees as determined by a laser altimeter. Each flight line was ~16 km and was completed in 5 min, and the whole grid operation took nearly 2 hours. The whole grid was flown twice in opposite directions. Each line was averaged into eight segments of 2 km each. This type of flight pattern, which was frequently flown in previous studies [*Desjardins et al*., 1992; *Mitic et al*., 1995; *Ogunjemiyo et al*., 1997], minimizes the effect of flux temporal variations since all segments were sampled at the same averaging time. A high-pass filtering routine was used in the segment flux calculation. The filter breakpoint was 0.005 and 0.010 Hz for 1994 and 1996 flux calculations, respectively [*MacPherson and Bastian*, 1997], corresponding to a cutoff wavelength of 12 and 6 km, respectively. It is found that this high-pass filtering technique produced more realistic segment fluxes than the linear detrending technique. The change in the filter breakpoint in 1996 is a minor refinement that causes 1–2% differences in the calculated fluxes under normal situations. The same data set was also used in the study of *Ogunjemiyo et al*. [1997] to produce flux maps within the grid. This filter does not remove any sporadic coherent vortices that induce abnormally large flux values [*MacPherson and Betts*, 1997]. These vortices, often occurring on scales smaller than a segment, could affect the inversion for a whole 16-km flight line when they occurred. However, the frequency of their occurrence was very low, i.e., nine events in a 16,000-km flight record [*MacPherson and Betts*, 1997], and would not have significantly affected the inversion results reported here.

2.2. Tower Flux Measurements

Several flux towers were erected for BOREAS in different forest species, named old black spruce (OBS), old jack pine (OJP), young jack pine (YJP), old aspen (OA), and fen. Figure 2 shows a typical 24-hour tower flux record on May 31, 1994, from the OBS site near Candle Lake in Saskatchewan, Canada. Most aircraft measurements during BOREAS field campaigns were taken between 1600 and 1900 UT (1100 to 1400 local time) when the mixed layer was highest and had the least temporal variation. During this time, flux divergence in the first 30 m is very small. Figure 2 shows a typical diurnal cycle of CO_2, positive (upward) at night because of respiration and negative (downward) during daytime when photosynthesis is larger than respiration. As the half-hourly tower measurements vary during the grid flight, the corresponding tower flux was averaged over the period of each aircraft grid flight.

2.3. Satellite Measurements

The land cover map covering SSA was produced from a Landsat thematic mapper (TM) image using bands 3 (red), 4 (infrared), and 5 (midinfrared) [*Hall et al*., 1997]. The original 11 cover types were regrouped and reduced into eight cover types to facilitate the use of aircraft data that were separated into eight segments for each flight line. The water cover type was not included in the analysis because it was almost nonexistent in the grid (<0.25%, see Table 1). Three regeneration classes (young, medium, and old) were combined into one because of their small percentage in the area. It is therefore reasonable to reduce the number of major cover types in this way. Otherwise, two lines have to be used for each inversion for more cover types. The final cover types used are (1) conifer wet (CW), (2) conifer dry (CD), (3) mixed (Mi) (coniferous and deciduous), (4) deciduous (De), (5) disturbed (Di), (6) fen (Fe), (7) regeneration (Re), and (8) visible burn (VB).

The dominant cover type in the boreal landscape is the black spruce, a wet conifer species. Plate 1 shows the color-coded land cover map of part of BOREAS SSA covering the flight grid. The spatial resolution of the map is 30 m. Three tower sites can be seen within the grid: OJP, YJP, and fen. OBS is located ~20 km west of the northwest corner of the grid (Figure 1). Figure 3 shows an example of aircraft CO_2 flux measurements during a single 16-km flight (leftmost line in Plate 1) with the CW area percentage in the quadrilateral box. Although CW is the dominant type, the CO_2 flux does not

Table 1. Daily Averages of the Pixel Percentage and Footprint-Weighted Area Percentage of the Different Cover Types in the Quadrilaterals Upwind of the Aircraft

	CW	CD	Mi	De	Di	Fe	Water	Re	VB
May 31, 1994, grid G									
pixel	69.66	0.75	14.64	0.48	0.12	7.74	0.02	6.53	0.06
footprint	61.47	3.71	12.87	2.22	1.12	5.96	···	12.60	0.06
June 4, 1994, grid G									
pixel	65.58	0.77	18.16	0.57	0.04	7.97	0.23	6.63	0.05
footprint	62.27	3.82	12.23	2.09	0.92	6.10	···	12.49	0.09
July 20, 1994, grid F									
pixel	66.80	0.65	17.07	0.58	0.08	8.01	0.10	6.67	0.05
footprint	58.53	4.79	12.10	2.18	1.32	6.39	···	14.52	0.16
July 21, 1994, grid G									
pixel	70.45	0.76	13.73	0.38	0.07	8.29	0.07	6.22	0.04
footprint	61.64	3.02	13.25	2.18	1.07	6.54	···	12.28	0.03
July 24, 1994, grid F									
pixel	67.21	0.67	16.63	0.57	0.06	8.05	0.09	6.11	0.05
footprint	58.62	4.93	11.86	2.08	1.32	6.50	···	14.53	0.16
July 26, 1994, grid G									
pixel	71.36	0.64	11.75	0.41	0.04	9.09	0.07	6.58	0.06
footprint	61.29	3.39	14.12	1.95	0.96	6.02	···	12.23	0.04
Sept. 16, 1994, grid G									
pixel	71.11	0.51	14.06	0.42	0.06	7.64	0.03	6.09	0.08
footprint	60.20	3.70	12.72	2.26	1.24	5.92	···	13.91	0.05
July 9, 1996, grid F									
pixel	58.62	3.63	11.57	2.20	1.29	7.82	0.08	14.72	0.06
footprint	57.46	5.48	10.82	2.04	1.41	6.76	···	15.89	0.13
July 20, 1996, grid F									
pixel	57.96	3.68	11.36	2.19	1.29	7.60	0.12	15.70	0.11
footprint	57.46	5.48	10.82	2.04	1.41	6.76	···	11.19	0.08
July 27, 1996, grid G									
pixel	60.95	2.82	11.89	2.00	1.12	6.99	0.12	14.06	0.03
footprint	62.08	3.19	12.63	1.67	0.92	7.16	···	13.87	0.07
July 29, 1996, grid F									
pixel	56.98	4.74	10.70	1.88	1.25	7.16	0.19	16.97	0.13
footprint	54.75	6.66	11.70	2.09	1.28	6.65	···	16.61	0.26

Quadrilaterals are shown in Plate 1. CW, conifer wet; CD, conifer dry; Mi, mixed; De, deciduous; Di, disturbed; Fe, fen; Re, regeneration; VB, visible burn.

seem to be well correlated with CW area percentage, indicating the influence of the other cover types. The quadrilateral boxes drawn on the side of the first flight line (Plate 1) represent footprint areas considered for each 2-km flight segment according to wind direction. In this case, the prevailing wind direction was west. The length of quadrilaterals is 5 km. According to our footprint calculations, under normal daytime atmospheric stability conditions, the area contributing 95% of fluxes is within 1 km upwind of an aircraft at 30 m from the displacement height. The same model was found to agree well with a trace gas release experiment in YJP and OJP [*Kaharabata et al*., 1997]. We used much larger areas to ensure that all pixels contributing to aircraft measurements are included. Pixels at different distances are given different weights according to a footprint function (see section 3.1).

3. Model Description

3.1. Linear Equations and Footprint Functions

The record of each 2-km segment of a flight line is influenced by fluxes from adjacent areas in the upwind direction. All cover types in the landscape can contribute to a downwind segment of a flux record depending on the area and distance from aircraft. In mathematical expression the following system of eight equations with eight unknowns can be established for the eight segments along a flight line:

$$\begin{aligned} C_{11}F_1 + C_{12}F_2 + \quad \cdots \quad + C_{18}F_8 &= F_{t1} \\ C_{21}F_1 + C_{22}F_2 + \quad \cdots \quad + C_{28}F_8 &= F_{t2} \\ \vdots \qquad\quad \vdots \qquad\quad \vdots \\ C_{81}F_1 + C_{82}F_2 + \quad \cdots \quad + C_{88}F_8 &= F_{t8} \end{aligned} \tag{1}$$

where F_{tk} is the aircraft-observed flux value of the kth segment along the line, C_{kj} is a weighting function for the jth land cover type and kth segment, and F_j is the spatially averaged flux density of jth cover type, which is unknown and is to be solved from (1). For different flight segments the weighting function C_{kj} for the same cover type can be different depending on the landscape and the wind direction. *Schuepp et al*. [1990] quantified the flux footprint from the contribution of an elemental area at a given distance in the upwind direction to a measured vertical flux at a fixed location. On the basis of their principles the following weighting function C'_{kj} is formulated:

$$C'_{kj} = \sum_{i=1}^{N} (n_{ij} w_i) \tag{2}$$

where i is the horizontal distance of a pixel in the upwind direction (expressed as the number of pixels from the aircraft in the upwind direction), w_i is the weight given to the pixel at the distance i upwind from the flight line, and n_{ij} is the number of pixels belonging to land cover type j at the distance i in a

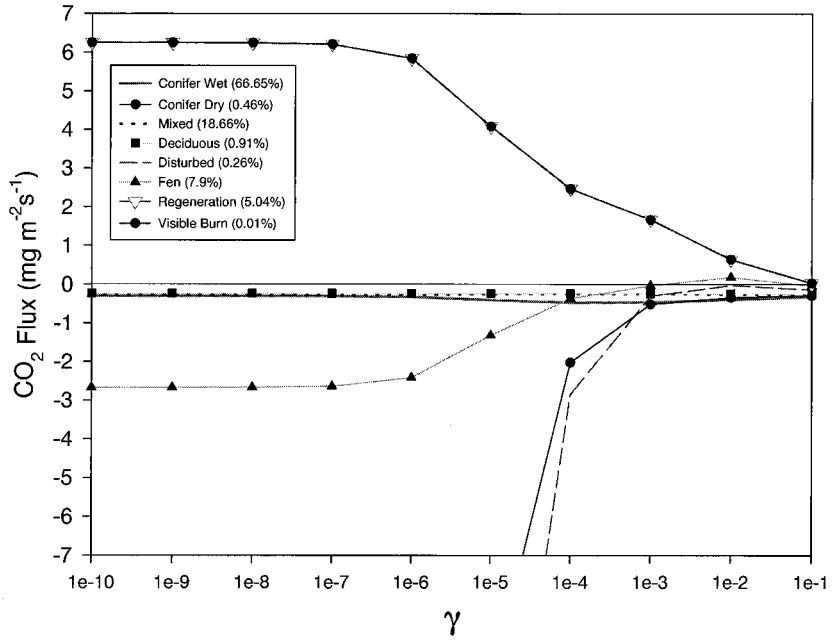

Figure 4. CO_2 flux calculated with the constrained linear least squares (CLLS) method for flight line 1, May 31, 1994, versus γ for the eight cover types, indicating the importance of numerical constraint in flux unmixing. Read 1e-10 as 1×10^{-10}.

row of pixels having the same length and parallel to the flight segment k. The length is made invariant with distance to reduce the complexity. This treatment can cause errors where the lateral mixing scales are >2 km. Such lateral mixing is unlikely because ~80% of fluxes generally occur within a few hundred meters of the aircraft at a height of 30 m under unstable conditions [*Kaharabata et al*., 1997]. Under the condition that the effective (80%) footprint area width for any given point in the flight segment is much smaller than the length of the flight segment, this two-dimensional footprinting approach is justified. Otherwise, the more complicated three-dimensional approach should be used [*Schmid and Oke*, 1990].

After normalization the weighting function becomes

$$C_{kj} = C'_{kj} \Big/ \sum_{j=1}^{8} C'_{kj} \tag{3}$$

The weight w_i is estimated from the footprint function [*Schuepp et al*., 1990; *Horst and Weil*, 1992]:

$$w_i = \frac{\Phi \dfrac{d\bar{z}}{dx}}{z_m} \tag{4}$$

where

$$\Phi = \begin{cases} A\left[\dfrac{z_m}{\bar{z}}\right]^2 e^{-z_m r/b\bar{z}} & u = \text{constant} \\ A\beta\left[\dfrac{z_m}{\bar{z}}\right]^2 e^{-z_m r/b\beta\bar{z}} & \text{for } u = u(z) \end{cases} \tag{5}$$

$$\frac{d\left(\dfrac{\bar{z}}{z_o}\right)}{d\left(\dfrac{x}{z_o}\right)} = \frac{k^2}{\left[\ln\left(p\,\dfrac{\bar{z}}{z_o}\right) - \psi\left(p\,\dfrac{z_o}{L}\,\dfrac{\bar{z}}{z_o}\right)\right]\phi_c\left(p\,\dfrac{z_o}{L}\,\dfrac{\bar{z}}{z_o}\right)} \tag{6}$$

where z_m is the measurement (flight) height; $\bar{z}$ is the mean plume height, which is a measure of vertical dispersion of a scalar at a given horizontal distance x from a surface source; u is the wind speed; z_o is the surface aerodynamic roughness; r is an exponent related to the atmospheric stability; k is von Karman constant; and b, A, and p are constants determined by r. In our model the following values are given [*Horst and Weil*, 1992, 1994]: $z_m = 30$ m, $z_o = 0.7$ m [*Kaharabata et al*., 1997], $r = 1.5$, $k = 0.4$, $b = 1.1515$, $A = 0.731$, and $p = 1.55$. The most important parameter, r, affecting several other parameters, is chosen to represent the neutral to moderately unstable atmospheric stability. For $L \geq 0$, where L is the Monin-Obukhov length,

$$\phi_c = \left[1 + 5p\,\frac{\bar{z}}{L}\right] \tag{7}$$

$$\psi = -5p\,\frac{\bar{z}}{L} \tag{8}$$

and for $L \leq 0$,

$$\phi_c = \left[1 + 16p\,\frac{\bar{z}}{L}\right]^{-1/2} \tag{9}$$

$$\psi = 2\ln\left[\frac{1+D}{2}\right] + \ln\left[\frac{1+D^2}{2}\right] - 2\tan^{-1}D + \frac{\pi}{2} \tag{10}$$

where

$$D = \left[1 - 16p\,\frac{\bar{z}}{L}\right]^{1/4} \tag{11}$$

and the stability

$$L = -\frac{u_*^3 T \rho C p}{kg(H + 0.07LE)} \tag{12}$$

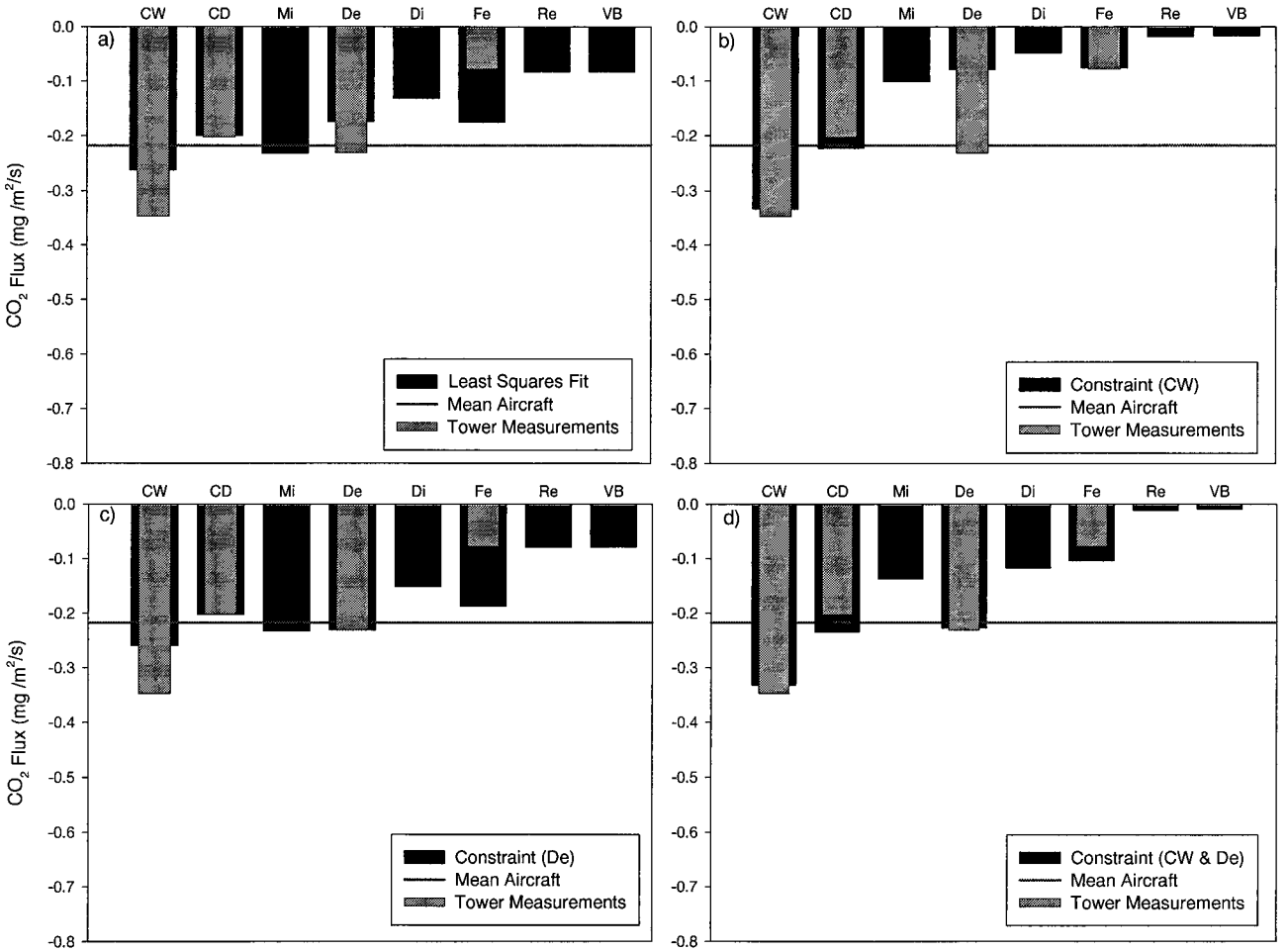

Figure 5. Unmixed CO_2 flux for May 31, 1994, using (a) CLLS method, (b) conifer wet (CW) forcing, (c) deciduous (De) forcing, and (d) CW and De forcings. The available simultaneous tower flux values are also shown for comparison.

where

$$u_* = \sqrt{\frac{|\tau|}{\rho}} \tag{13}$$

In the above, T is the air temperature (K) measured at the aircraft height, H and LE are the sensible and latent heat fluxes (W m^{-2}) measured at the aircraft, $Cp = 1005$ J (kg K)$^{-1}$ is the specific heat, $\rho = 1.19$ kg m^{-3} is the air density, $g = 9.8$ m s^{-2} is the acceleration due to gravity, and τ is the momentum flux (N, or kg m^{-1} s^{-2}) measured by the aircraft. At $x = z_o$ we assume that $\bar{z} = z_o$. The mathematical scheme and the values for the parameters used are all adopted without modification from *Horst and Weil* [1992]. Identical footprint distributions like those shown by Horst and Weil were obtained using our own code.

3.2. Solving the Equation System: Linear Inversion Methods

Equation (1) can be rewritten in a matrix form as

$$\mathbf{CF} = \mathbf{F_t} \tag{14}$$

where $\mathbf{F_t}$ is the vector containing the aircraft flux measurements, $\mathbf{C}$ is the matrix with the weighting (footprint) coefficients, and $\mathbf{F}$ is the vector of unknown fluxes from different cover types. Equation (14) can be solved directly as follows:

$$\mathbf{F} = \mathbf{C^{-1}F_t} \tag{15}$$

Since any errors in the measurements of $\mathbf{F_t}$, in the collocation of flight lines in the land cover map, and in footprint calculations due to within-segment wind direction variations affect subsequent calculations, (15) can sometimes give results out of the range of possibility. Even a small measurement error can be amplified in the inversion because of the large values of $\mathbf{C^{-1}}$. Inversion stability can be improved using a numerical constraint that confines the solution within a certain physically realistic range. Different constraints based on knowledge of the physics involved or on previous measurements or constraints used as a smoothing technique can be applied. One method is the constrained linear least squares (CLLS) [*Twomey*, 1977; *Perry et al.*, 1988]. The CCLS method is used to find, out of many possible solutions from the data, the one that satisfies a prescribed constraint. This is done by minimizing $\mathbf{q}$, which represents the departure from the constrained solution, while making sure that $(\mathbf{CF} - \mathbf{F_t})^2 < \varepsilon^2$. Replacing the inequality with $(\mathbf{CF} - \mathbf{F_t})^2 = \varepsilon^2$, the Lagrange multipliers method can be used. In this case, ε represents the residual of the solution. The optimization is done by finding the minimum of $(\mathbf{CF} - \mathbf{F_t})^2 + \gamma\mathbf{q}$:

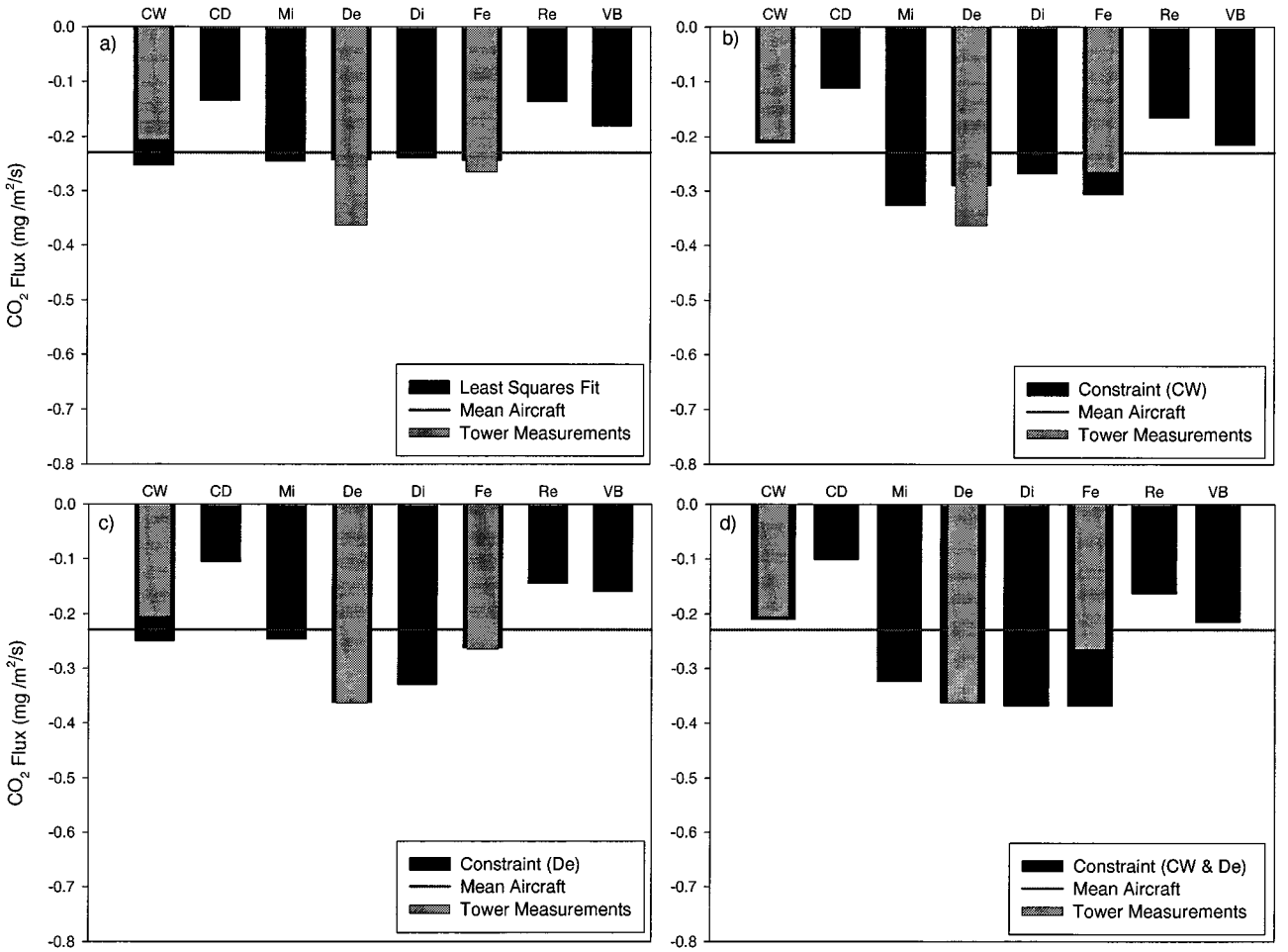

Figure 6. Unmixed CO_2 flux for June 4, 1994, using (a) CLLS method, (b) CW forcing, (c) De forcing, and (d) CW and De forcings.

$$\frac{\partial}{\partial F_k}[(\mathbf{CF} - \mathbf{F_t})^T(\mathbf{CF} - \mathbf{F_t}) + \gamma\mathbf{q}] = 0 \tag{16}$$

where γ is a Lagrange multiplier. If the behavior of the resulting $\mathbf{F}$ is not known, the constraint can be used to force a smoothed solution. To use a least squares method with constraints, the following constraint matrix is introduced:

$$\mathbf{H} = \begin{bmatrix} 1 & -1 & 0 & 0 & 0 & 0 & 0 & 0 \\ -1 & 2 & -1 & 0 & 0 & 0 & 0 & 0 \\ 0 & -1 & 2 & -1 & 0 & 0 & 0 & 0 \\ 0 & 0 & -1 & 2 & -1 & 0 & 0 & 0 \\ 0 & 0 & 0 & -1 & 2 & -1 & 0 & 0 \\ 0 & 0 & 0 & 0 & -1 & 2 & -1 & 0 \\ 0 & 0 & 0 & 0 & 0 & -1 & 2 & -1 \\ 0 & 0 & 0 & 0 & 0 & 0 & -1 & 1 \end{bmatrix} \tag{17}$$

The solution is found by solving (16) with the constraint $\mathbf{H}$ so that $\mathbf{q} = \mathbf{F}^T\mathbf{HF}$. Equation (16) becomes

$$\frac{\partial}{\partial F_k}[(\mathbf{CF} - \mathbf{F_t})^T(\mathbf{CF} - \mathbf{F_t}) + \gamma\mathbf{F}^T\mathbf{HF}] = 0 \tag{18}$$

and the solution of (18) is

$$\mathbf{F} = (\mathbf{C}^T\mathbf{C} + \gamma\mathbf{H})^{-1}\mathbf{C}^T\mathbf{F_t} \tag{19}$$

Equation (19) is a general solution and depends on the γ value. The final γ values should give a residual ε not larger than the total error in the data, which is assumed to be 10%. In final calculations made in this paper, γ values are always <0.3, causing a maximum 1% departure of the total inverted fluxes from the aircraft measurements.

A flexibility of the constrained calculation can be introduced in order to use any available ground (tower) measurements as part of the constraint. For this purpose, (19) can be changed to

$$\mathbf{F} = (\mathbf{C}^T\mathbf{C} + \gamma\mathbf{H} + \mathbf{S})^{-1}(\mathbf{C}^T\mathbf{F_t} + \mathbf{T}) \tag{20}$$

where $\mathbf{S}$ is a matrix where the diagonal elements are the known tower values multiplied by given weighting factors and $\mathbf{T}$ is a vector containing the observed flux at the towers times the weighting factor and zero elsewhere. Large weighting factors for given cover types can force the solution to be very close to the tower measurements for the same cover types. A weighting factor of 10 was used for all available tower measurements in this study, which is a convenient number to use since the constrained inversion is not sensitive to this value when it is >5.

The same unmixing and constraining principles described above can be used in other measurement or processing schemes. For example, each 16-km flight line can be used as a segment instead of a 2-km segment. We choose to use the 2-km segments because they are already much longer than the ef-

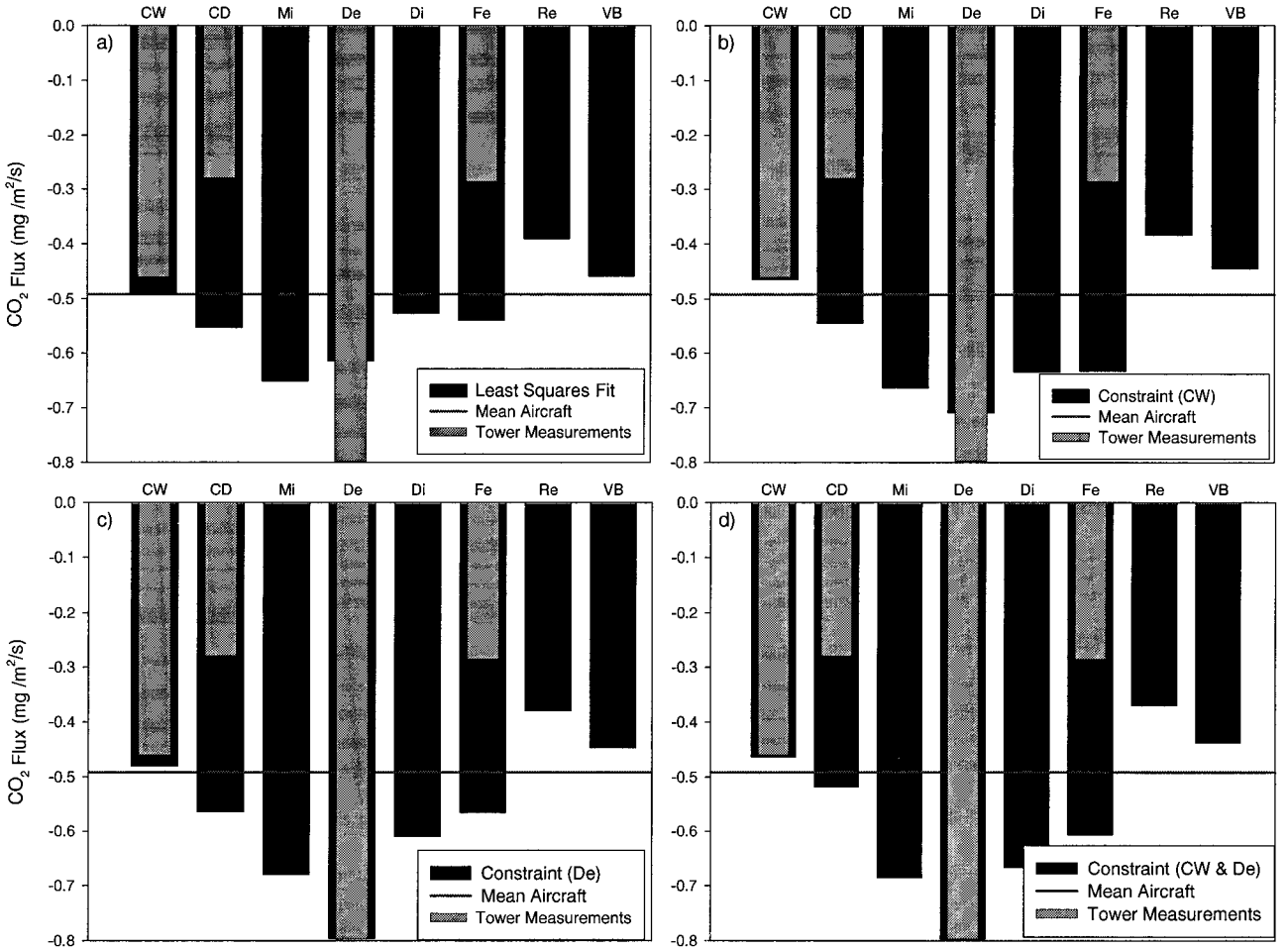

Figure 7. Unmixed CO_2 flux for July 20, 1994, using (a) CLLS method, (b) CW forcing, (c) De forcing, and (d) CW and De forcings.

fective (80%) length of the footprint area, which is generally only a few hundred meters [*Kaharabata et al.*, 1997]. The timescale for turbulent gas diffusion from the surface to the aircraft at z_m can be estimated as z_m/u_* within the surface layer [*Stull*, 1988], which is ~30–100 s, meaning that the measurements taken at the aircraft were not instantaneous fluxes from the surface but were representative of about a minute ago. It took the aircraft about 35 s to complete a 2-km segment at the speed of 200 km h^{-1}. Since the wind direction measured on board for each segment was used, an error in the footprint calculations can occur if the mean wind direction changes considerably from one minute to the other. In some cases, an improvement may be made by averaging, for each segment, the wind direction for several adjacent segments having a total lapse time similar to the diffusion time (0.5–1.5 min). In our case, it would be an average of 1–3 segments, and therefore our choice of using single-segment wind direction is reasonable. An alternative is to use longer flight segments. However, if the segments are too long and the area fractions of the underlying cover types become too similar among segments, the numerical inversion becomes more unstable, and stronger constraints are needed. The choice of the segment length is therefore an important technical issue. The decision should be made on the basis of the atmospheric stability, flight height, surface roughness, wind variability, and the scale of surface heterogeneity. We believe that the 2-km segment length used in this study is close to the optimum, but further studies are required to quantify systematically the effect of segment choice on inversion results under various conditions.

4. Results and Discussion

4.1. Flux Unmixing

Seven cases (days) from May 31 to September 16, 1994, and four cases in July 1996 were analyzed with the method described in section 3.2. The CLLS inversion method was initially used to test the value of the methodology based on aircraft measurements only. Equation (19) was applied to each flight line separated into eight segments. The value of γ was increased logarithmically from 10^{-20} until all cover types fluxes were found between -1 and 0.1 mg CO_2 m^{-2} s^{-1}. When the order of magnitude of γ was found in this way, the precise γ value within the order required to bring all flux values to the range was determined in a small linear step. Results from the 18 lines are reported here as arithmetic means of all cover types. As changes in the major cover type fractions are small between flight lines, only very small improvements are found from a weighted average using the percentage of each cover type for each flight line. Table 1 shows the average cover fractions in the 2 km × 5 km footprint quadrilaterals and the

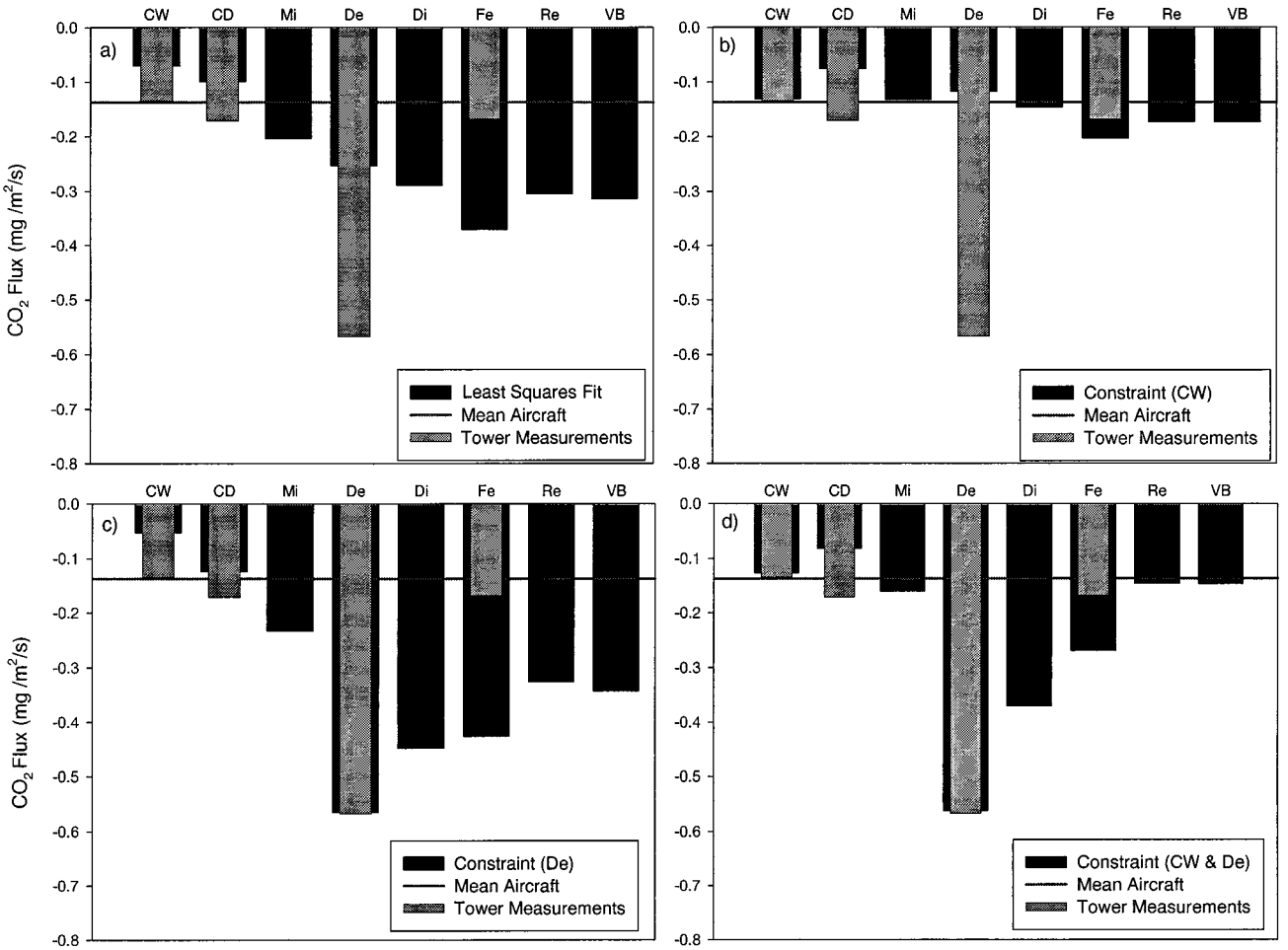

Figure 8. Unmixed CO_2 flux for July 21, 1994, using (a) CLLS method, (b) CW forcing, (c) De forcing, and (d) CW and De forcings.

footprint-weighted cover fractions for all flight days. The fractions differ between flight lines and from day to day because of changes in wind direction and flight line location. The conifer wet (CW) has by far the largest fraction, and the next significant cover types in order of importance are the regeneration (Re), mixed (Mi), fen (Fe), and conifer dry (CD). The small lakes, which occupied only very small areas, are ignored.

Figure 4 shows how the constraint affects calculated fluxes as γ increases. For γ values near zero the two dominant cover types, the mixed (18.66% of the pixels) and conifer wet (66.65%), are shown with reasonable flux values. The small cover types, except for De in this case, have values beyond the physically possible range with or without weak constraint. The fluxes of the various cover types converge toward reasonable values for γ between 0.001 and 0.1. All the fluxes were forced between -1 and 0.1 mg CO_2 m^{-2} s^{-1} when γ is increased to 0.08. Figure 4 demonstrates that a mathematical constraint is a prerequisite for the flux unmixing using the least squares inversion method and that the simple constraining method using a fixed constraining matrix and a variable γ value is effective in confining the calculated values to a prescribed range. However, in this way, the flux values of the various cover types depend on the γ values used, and a subjective influence on the results cannot be avoided. The magnitude of errors in aircraft flux measurements can be used to find the maximum allowable γ value because the departure of the total calculated fluxes from the aircraft measurements increases as the γ value increases. For the 18 lines in a flight grid the departure of the sum of the fluxes is always $<1\%$ from the measured mean aircraft flux, indicating that the constraining was weak to moderate for all cases. This simple constraining method without assistance of ground data can produce reasonable values for cover types with significant coverage, but errors for some infrequent cover types can be large, and the constraint tends to be excessive in order to bring all cover types within a reasonable range. In doing so, the difference between fluxes of the major cover types may be unnecessarily compressed. This problem of "blind constraint" can be reduced or avoided when other independent measurements, such as tower flux data, are available for some or all cover types involved. In general, measurements for only some cover types are available, and (20) is useful for this purpose.

When tower measurements are used in the constraint, we implicitly assume that these measurements represent the cover types in which they were made. This seems to contradict one of the objectives of this study, i.e., to assess the representativeness of tower measurements using aircraft data because many sources of measurement errors can cause large differences between aircraft and tower measurements [*Mahrt*, 1998]. However, the total inversion error after constraint can be used to

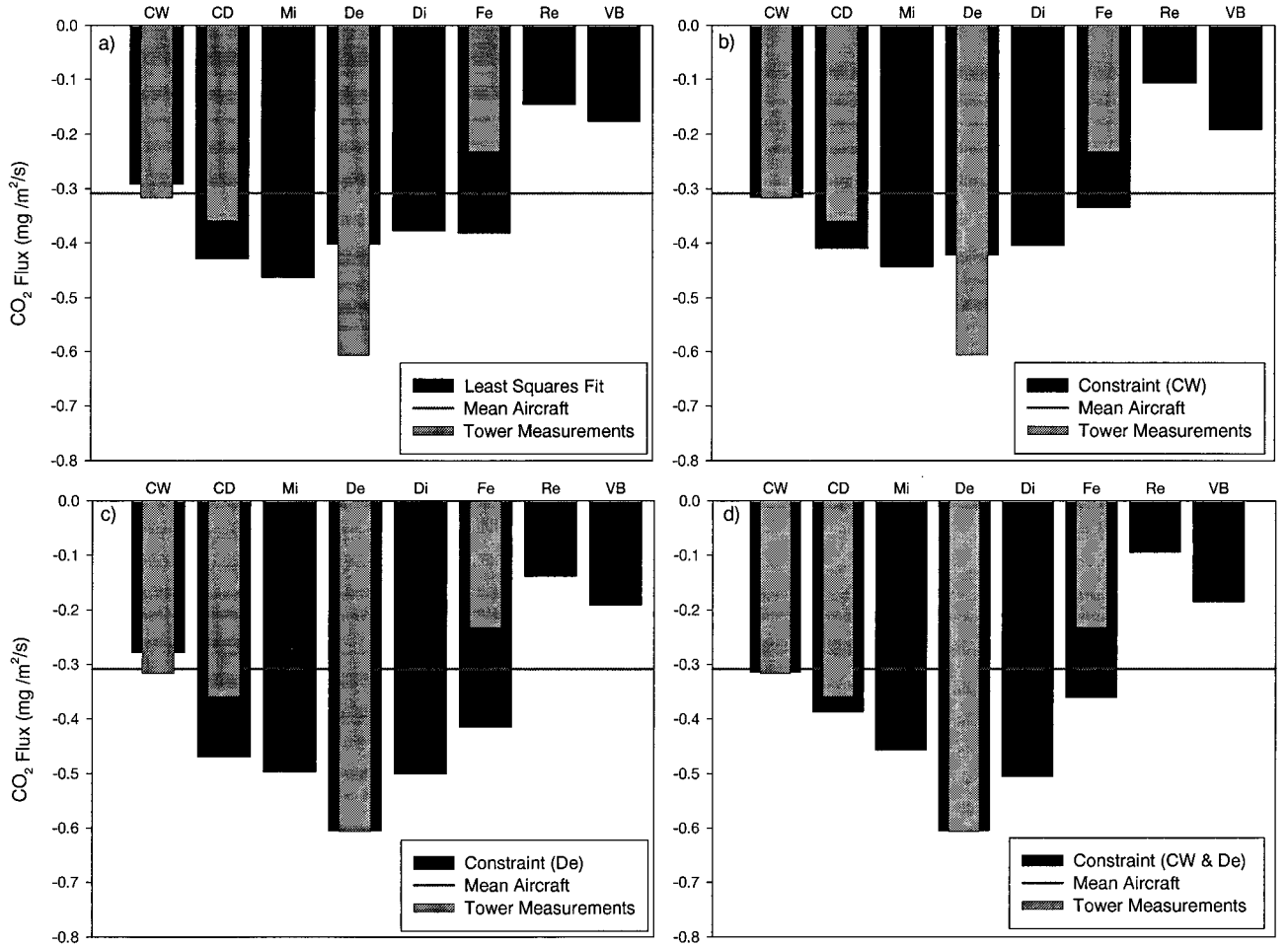

Figure 9. Unmixed CO_2 flux for July 24, 1994, using (a) CLLS method, (b) CW forcing, (c) De forcing, and (d) CW and De forcings.

gage the representativeness of some tower measurements. For example, if a flight line is totally occupied by a cover type and the aircraft flux measurements differ from the tower measurements, the inversion error is the difference between tower and aircraft measurements even though the inverted flux is made equal to the tower value through a strong constraint. Since wet conifer is the predominant cover type, the representativeness of the wet conifer can then be found from the error in the constrained inversion represented by the size of the γ value necessary to bring all the inverted results to a prescribed range. The mixed cover type is composed of conifer and deciduous types, and therefore it is expected that its flux should be between those of conifer and deciduous cover types. It therefore also provides useful information for assessing the representativeness. These concepts may be illustrated in the following examples in 1994 when five simultaneous tower measurements for four cover types were available (old jack pine and young jack pine tower measurements were combined for the CD type).

On May 31, 1994, the OBS tower had a flux considerably larger than the mean aircraft flux measurement. Figure 5a shows that the CLLS method cannot produce a mean CW flux comparable to the OBS tower measurements. After forcing the CW to the OBS tower flux the difference is much reduced (Figure 5b). A β value larger than 10 is needed to further reduce the difference. Because of the large change in CW flux after the forcing, which also causes large changes in other cover types, a large γ value of 0.259 (0.068 in the CLLS case) was needed to bring all other cover types to within the prescribed range. Forcing only the deciduous flux to the OA tower measurement (Figure 5c) does not cause the required γ value to change much from the CLLS case because of its small area fraction. The CW forcing causes large reductions in many cover types, making the Mi flux, especially, very small, indicating that the OBS tower flux was likely larger than that of CW in the flight grid. However, the calculated flux from the Fe type agrees with the tower measurements only after the CW forcing, suggesting that the Fe tower measurements were also larger than the grid average in this case. CD was in agreement with the tower measurement and was not much affected by the various constraint methods. On June 4, 1994, the CLLS method (Figure 6a) produces good agreement between the OBS and fen tower measurements and the calculated fluxes from the aircraft, although De is underestimated by the aircraft. Figure 6b shows that the CW forcing to the smaller tower values causes the downward fluxes of all cover types except CD to increase. On July 20, 1994, the four methods give similar results as seen in Figure 7. The mixed cover type flux is found in between CW and De values obtained from the towers. The case on July 21, 1994 (Figure 8), shows very small flux values

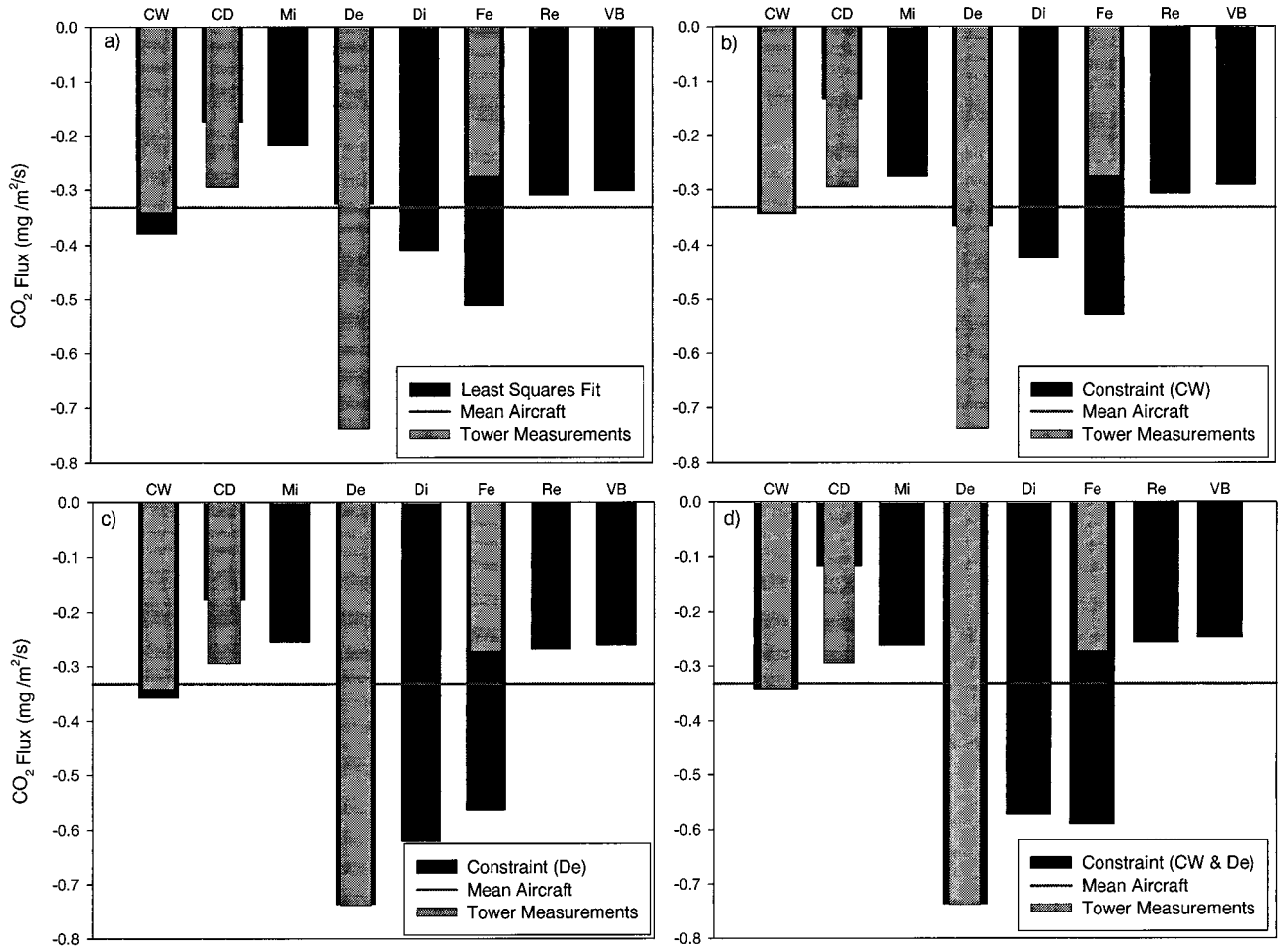

Figure 10. Unmixed CO_2 flux for July 26, 1994, using (a) CLLS method, (b) CW forcing, (c) De forcing, and (d) CW and De forcings.

measured by the aircraft and by three of the four towers. The OA tower flux is very large in comparison with the other tower fluxes, but since the region contains only a small percentage of deciduous pixels, its influence was very small on the aircraft fluxes and on the inversion of fluxes of other cover types. The CLLS method (Figure 8a) produces a CW flux smaller than the OBS tower measurement. The days of July 24 and 26, 1994 (Figures 9 and 10), are two examples of CLLS results for CW being very close to the OBS tower measurements. Only very small constraints are needed in these two cases. However, Fe results under the various constraints are always larger than the fen tower measurement. On September 16, 1994, the OBS tower flux is considerably larger than the mean aircraft flux (Figure 11). The calculations for this day clearly represent how forcing to a tower measurement that deviates largely from the aircraft mean value affects the unmixing results. After a strong CW forcing with a large γ of 0.249 the fluxes of cover types with significant areas are much reduced because the change in one cover type must be compensated by other cover types. It is shown again that OBS tower measurements were positively biased (too large a downward flux) because CW forcing makes the flux of all other cover types, except CD, unreasonably small.

From the above cases, we can qualitatively see the following: (1) The tower measurements for the Fe type were often negatively biased (too small a downward flux) compared to aircraft-derived values. (2) OBS tower measurements were strongly positively biased on days when the aircraft-measured downward flux was small. (3) The aircraft-inverted De fluxes are often too small compared with OA tower fluxes because the fraction of De cover in the flight grid is too small (~2%). On some days (May 31, July 21, July 24, and September 16) we can infer that OBS tower measurements were larger than the average CW value for the grid from the facts that CLLS results for CW were smaller than OBS tower measurements and that CW forcing often causes the mixed type flux to be unrealistic (smaller than CW when the deciduous type has flux values larger than conifer). On other days (mostly when the downward flux was large) the OBS tower measurements appear to be representative of the CW type. It is shown that the representativeness of tower measurements can be assessed from the response of other cover types to the constraint using the measurements. We are not yet able to determine the causes for the aircraft-derived flux for the Fe type being consistently larger than the fen tower measurements. The results must depend, to some extent, on the accuracy of the land cover map and the definition of fen.

All results of unmixing for 1994 and 1996 using the four constraining methods are given in Table 2. To quantify the goodness of fit, statistical analysis of the calculated fluxes is

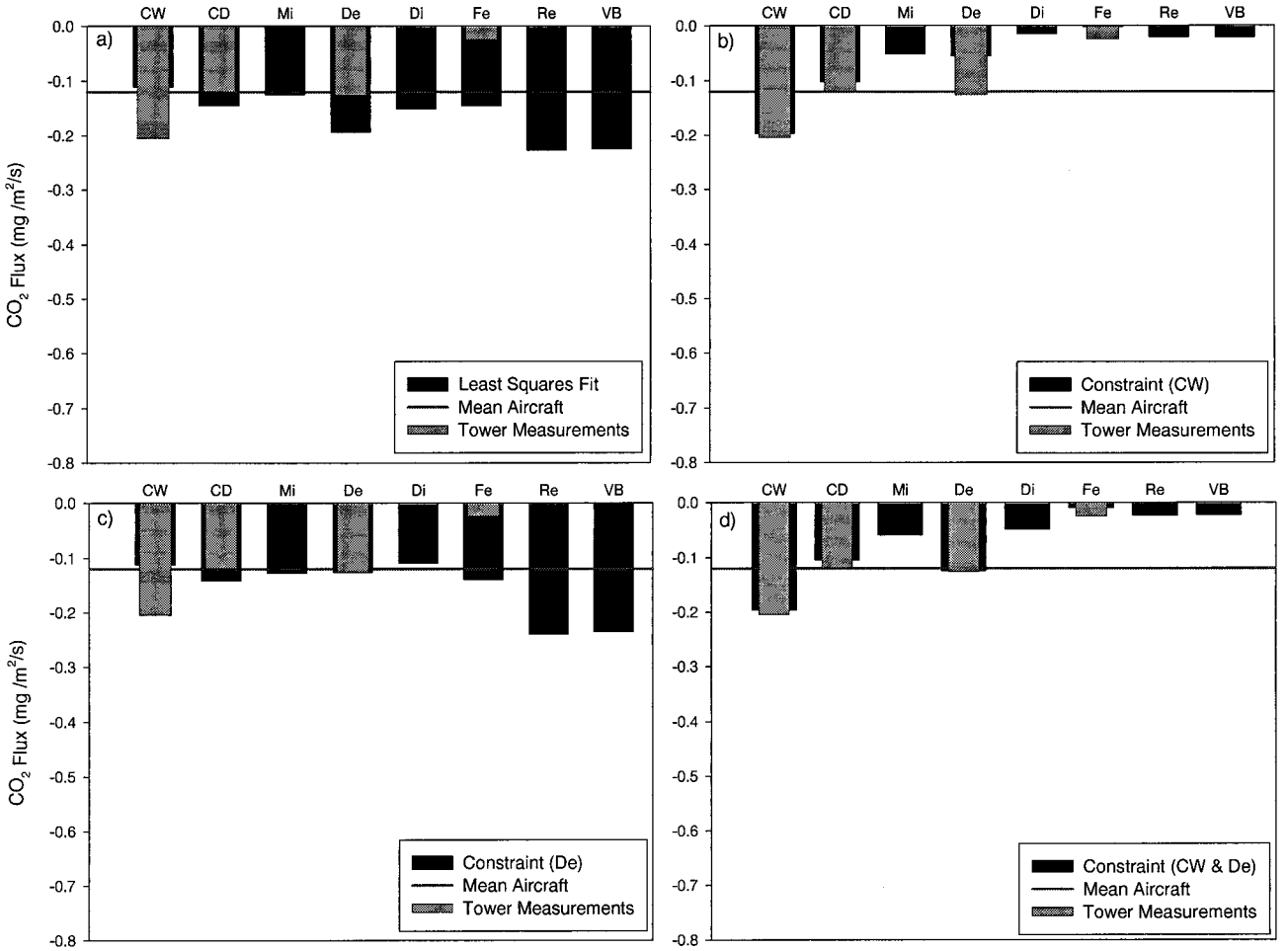

Figure 11. Unmixed CO_2 flux for September 16, 1994, using (a) CLLS method, (b) CW forcing, (c) De forcing, and (d) CW and De forcings.

made against tower measurements, assuming all towers were representative (Table 3). Figure 12a compares the aircraft-based fluxes with tower-based fluxes without using ground measurements in the constraint. For wet and dry conifers and fen the CLLS produces reasonably good results (R^2 = 0.73, 0.45, and 0.65 for these three cover types, respectively). This confirms that the unmixing method using aircraft measurements alone can produce reasonable estimates for cover types with significant coverage (>5%). For the deciduous cover type (R^2 = 0.38), the fluxes of six of the ten days were underestimated, one was overestimated, and the fluxes on the three other days were very close to tower data. Figures 12b–12d show how the tower constraints affect the goodness of fit. The use of tower constraints improves the results for the constrained cover types but also affects some unconstrained cover types considerably. Figure 12b shows that calculated values for wet conifer under the OBS tower constraint improve from an R^2 of 0.73 to an R^2 of 0.99. This is expected because of the large degree of forcing used (β = 10). However, the major improvement brought about by this constraint is in the calculated values for Fe: The overall coefficient of determination R^2 increased from 0.65 to 0.83. The calculation for Fe was affected by the constraint on the wet conifer because fen has significant coverage (5–7%). The same constraint has little effect on dry conifer because of the small coverage (2–5%). When tower measurements from the OA site were used as the only constraint, the Fe cover type is not much affected (R^2 = 0.65), and neither are the other cover types (Figures 12c and 12d). This is because the deciduous type only makes up ~2% of the total coverage. Using both wet conifer and deciduous constraints does not further improve the calculation for the fen from the case of wet conifer constraint only. Dry conifer is not much affected by any constraint combinations because of the small coverage. The fen results are greatly improved by the wet conifer constraint, but the fen tower measurements are consistently smaller than the aircraft-inverted value. However, overall, the partial constraining method using limited tower measurements appears to be effective.

One caution should be taken in interpreting the unmixing results: The spatial distribution patterns of the various cover types should be independent of each other along the wind direction. If two cover types always appear consecutively in the direction of gas dispersion, they become difficult to differentiate. This spatial correlation problem was found to exist between disturbed and deciduous cover types. Disturbed areas are mostly roads and built-up areas, and they are often found to be close to deciduous forests. Disturbed areas are therefore erroneously found in the inversion to have large flux values similar to the deciduous forests. In such a case, some constraint is needed for the disturbed type. This can be done by assigning

Table 2. Unmixed CO_2 Flux Values Obtained With Four Constraint Methods and the γ Values and Tower Measurements From the Old Black Spruce, Old and Young Jack Pines, Old Aspen, and Fen Sites

	CW	CD	Mi	De	Di	Fe	Re	VB	γ
May 31, 1994									
CLLS	−0.262	−0.200	−0.232	−0.174	−0.132	−0.175	−0.083	−0.083	0.068
CW	−0.333	−0.223	−0.101	−0.078	−0.048	−0.075	−0.018	−0.016	0.259
De	−0.260	−0.203	−0.233	−0.231	−0.151	−0.187	−0.079	−0.078	0.053
CW-De	−0.331	−0.234	−0.137	−0.227	−0.117	−0.104	−0.011	−0.009	0.245
tower	−0.347	−0.203	···	−0.231	···	−0.078	···	···	···
June 4, 1994									
CLLS	−0.253	−0.134	−0.245	−0.242	−0.239	−0.243	−0.136	−0.180	0.080
CW	−0.211	−0.111	−0.326	−0.289	−0.268	−0.305	−0.164	−0.214	0.019
De	−0.249	−0.105	−0.246	−0.362	−0.329	−0.262	−0.145	−0.159	0.041
CW-De	−0.210	−0.101	−0.323	−0.362	−0.368	−0.368	−0.162	−0.214	0.018
tower	−0.205	···	···	−0.363	···	−0.265	···	···	···
July 20, 1994									
CLLS	−0.493	−0.552	−0.651	−0.614	−0.526	−0.539	−0.390	−0.458	0.141
CW	−0.464	−0.545	−0.663	−0.709	−0.634	−0.633	−0.383	−0.444	0.108
De	−0.480	−0.564	−0.680	−0.796	−0.610	−0.566	−0.380	−0.447	0.113
CW-De	−0.464	−0.518	−0.685	−0.797	−0.667	−0.607	−0.370	−0.438	0.087
tower	−0.460	−0.279	···	−0.797	···	−0.285	···	···	···
July 21, 1994									
CLLS	−0.070	−0.099	−0.203	−0.253	−0.288	−0.370	−0.304	−0.313	0.056
CW	−0.131	−0.076	−0.133	−0.117	−0.146	−0.202	−0.173	−0.173	0.066
De	−0.052	−0.124	−0.233	−0.565	−0.448	−0.426	−0.326	−0.342	0.060
CW-De	−0.126	−0.081	−0.161	−0.563	−0.370	−0.269	−0.146	−0.147	0.079
tower	−0.135	−0.171	···	−0.567	···	−0.168	···	···	···
July 24, 1994									
CLLS	−0.291	−0.429	−0.463	−0.402	−0.377	−0.381	−0.145	−0.176	0.057
CW	−0.316	−0.409	−0.443	−0.422	−0.404	−0.334	−0.107	−0.192	0.024
De	−0.278	−0.469	−0.497	−0.605	−0.500	−0.415	−0.138	−0.192	0.050
CW-De	−0.314	−0.387	−0.457	−0.605	−0.505	−0.360	−0.094	−0.185	0.041
tower	−0.316	−0.359	···	−0.606	···	−0.232	···	···	···
July 26, 1994									
CLLS	−0.378	−0.175	−0.217	−0.325	−0.409	−0.511	−0.309	−0.302	0.039
CW	−0.343	−0.132	−0.274	−0.365	−0.424	−0.528	−0.306	−0.291	0.019
De	−0.358	−0.177	−0.256	−0.736	−0.621	−0.563	−0.269	−0.261	0.028
CW-De	−0.341	−0.117	−0.263	−0.737	−0.572	−0.589	−0.257	−0.248	0.024
tower	−0.341	−0.295	···	−0.738	···	−0.273	···	···	···
Sept. 16, 1994									
CLLS	−0.110	−0.145	−0.124	−0.194	−0.150	−0.145	−0.227	−0.225	0.070
CW	−0.197	−0.102	−0.051	−0.055	−0.015	−0.002	−0.020	−0.021	0.249
De	−0.112	−0.141	−0.127	−0.126	−0.109	−0.139	−0.239	−0.235	0.053
CW-De	−0.196	−0.104	−0.059	−0.124	−0.048	−0.010	−0.023	−0.022	0.192
tower	−0.205	−0.119	···	−0.126	···	−0.025	···	···	···
July 9, 1996									
CLLS	−0.281	−0.443	−0.618	−0.502	−0.495	−0.445	−0.220	−0.205	0.063
CW	−0.344	−0.363	−0.513	−0.473	−0.418	−0.328	−0.197	−0.181	0.059
De	−0.265	−0.464	−0.619	−0.750	−0.623	−0.505	−0.199	−0.197	0.040
CW-De	−0.342	−0.362	−0.512	−0.749	−0.564	−0.337	−0.191	−0.185	0.053
tower	−0.349	···	···	−0.751	···	···	···	···	···
July 20, 1996									
CLLS	−0.372	−0.445	−0.614	−0.503	−0.394	−0.335	−0.259	−0.261	0.138
CW	−0.332	−0.493	−0.654	−0.582	−0.516	−0.431	−0.295	−0.291	0.094
De	−0.347	−0.424	−0.656	−0.779	−0.526	−0.404	−0.275	−0.282	0.136
CW-De	−0.347	−0.424	−0.656	−0.779	−0.526	−0.404	−0.275	−0.282	0.136
tower	−0.328	···	···	−0.782	···	···	···	···	···
July 27, 1996									
CLLS	−0.434	−0.504	−0.442	−0.431	−0.384	−0.372	−0.374	−0.403	0.103
CW	−0.368	−0.496	−0.528	−0.607	−0.530	−0.514	−0.379	−0.379	0.073
De	−0.462	−0.491	−0.393	−0.029	−0.133	−0.270	−0.370	−0.409	0.112
CW-De	−0.374	−0.519	−0.517	−0.032	−0.206	−0.412	−0.334	−0.336	0.112
tower	−0.361	···	···	−0.022	···	···	···	···	···
July 29, 1996									
CLLS	−0.430	−0.353	−0.510	−0.540	−0.361	−0.339	−0.155	−0.188	0.045
CW	−0.320	−0.418	−0.728	−0.667	−0.550	−0.506	−0.237	−0.272	0.036
De	−0.421	−0.337	−0.564	−0.655	−0.471	−0.344	−0.146	−0.178	0.035
CW-De	−0.320	−0.367	−0.744	−0.656	−0.554	−0.488	−0.237	−0.268	0.029
tower	−0.309	···	···	−0.656	···	···	···	···	···

The constraint methods include the following: constrained linear least squares (CLLS), CW forcing, De forcing, and CW-De forcings. The old black spruce site is CW, the old and young jack pines sites are CD, and the old aspen site is De.

Table 3. Coefficient of Determination R^2 of Unmixed Fluxes Obtained With the Four Constraint Methods Versus the Measurements of Old Black Spruce, Old Aspen, Old and Young Jack Pines, and Fen Tower Sites

	OBS-CW	JP-CD	OA-De	Fen
CLLS	0.73	0.45	0.38	0.65
OBS	0.99	0.43	0.22	0.83
OA	0.72	0.49	1.00	0.65
OBS-OA	0.99	0.39	1.00	0.90

The constraint methods include the following: CLLS, CW forcing, De forcing, and CW-De forcings. OBS, old black spruce; JP, jack pine; OA, old aspen.

an appropriate flux value within the constraint matrix. Since the fraction of the disturbed areas is small, the inversion results for other cover types are not sensitive to the chosen value for this cover type. Another example of the spatial adjacency effect is between CW and Fe. Because they are often located close to each other, CW forcing causes changes in Fe more often than in other cover types. However, this effect is expected to be small because of the significant area fraction of Fe and the similarity in flux between these two types (both from tower and aircraft).

4.2. Scaling From Line to Region

The ultimate goal of our analysis of aircraft CO_2 flux measurements is to obtain regional estimates of the flux. The major steps involved in achieving the goal include (1) overlaying flight lines within a land cover map, (2) obtaining the average fluxes for all cover types in the region through flux unmixing, and (3) calculating the average regional flux using unmixing results and the fractions of all cover types in the region. The first two steps are completed in the section above, and the third is straightforward. However, some questions still remain: (1) Can we unmix the aircraft flux without the assistance of tower

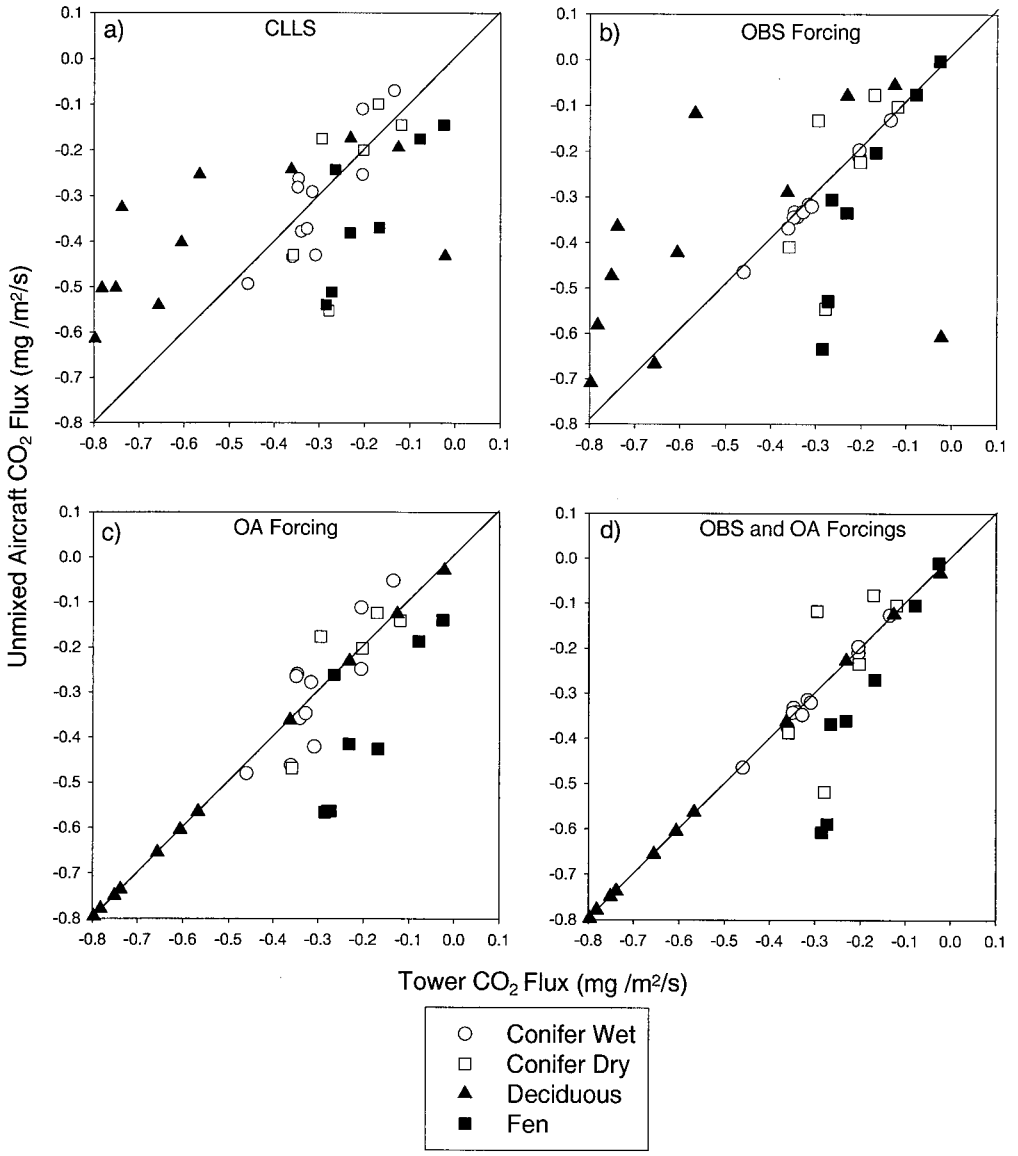

Figure 12. Scatterplots of all simultaneous tower CO_2 fluxes in 1994 and 1996 compared with the unmixed aircraft fluxes: (a) CLLS method, (b) CW forcing, (c) De forcing, and (d) CW and De forcings. The diagonal lines are one-to-one lines. The coefficients of determination for different cover types are given in Table 3.

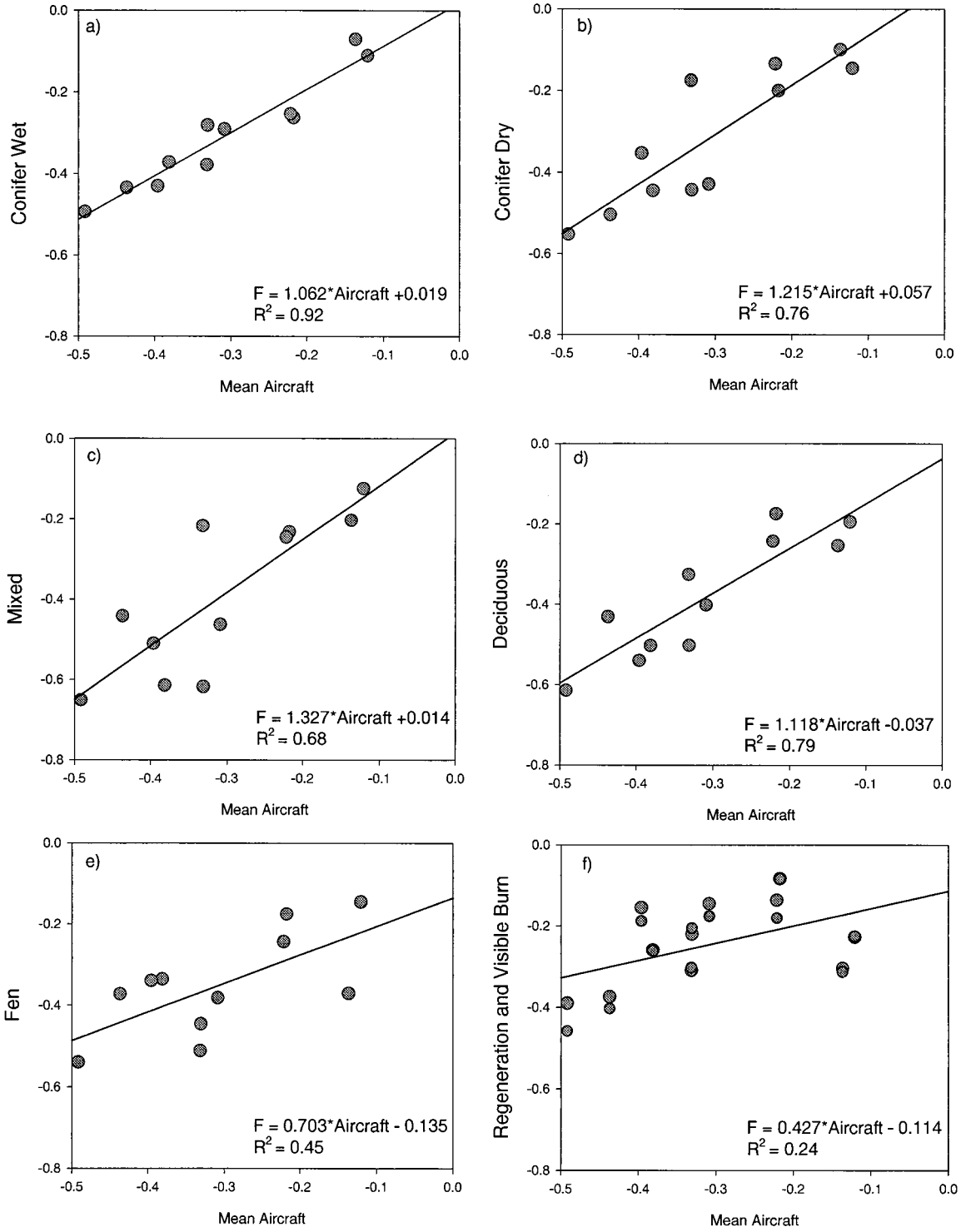

Figure 13. Linear relationship between the mean aircraft CO_2 flux (mg m^{-2} s^{-1}) in 1994 and 1996 and the unmixed flux obtained using the CLLS method for the main cover types: (a) conifer wet, (b) conifer dry, (c) mixed, (d) deciduous, (e) fen, and (f) regeneration and visible burn.

data? (2) How can aircraft measurements, made at limited times and on limited days, be used to assist in regional flux estimation on other times and days?

Figures 13 and 14 are presented in the attempt to address these questions. Figure 13 shows the relationship between the aircraft mean flux for a complete grid flight and the mean fluxes for the various cover types obtained using the CLLS method without any ground data (disturbed type is not shown because of its small area fraction). Figure 14 shows similar relationships obtained under the CW and De tower constraints. The slope, intercept, and the R^2 value in Figures 13 and 14 may be used as guidelines to understand the effects of tower constraint on upscaling. The slope is related to the productivity (flux density) since the intercept should generally be

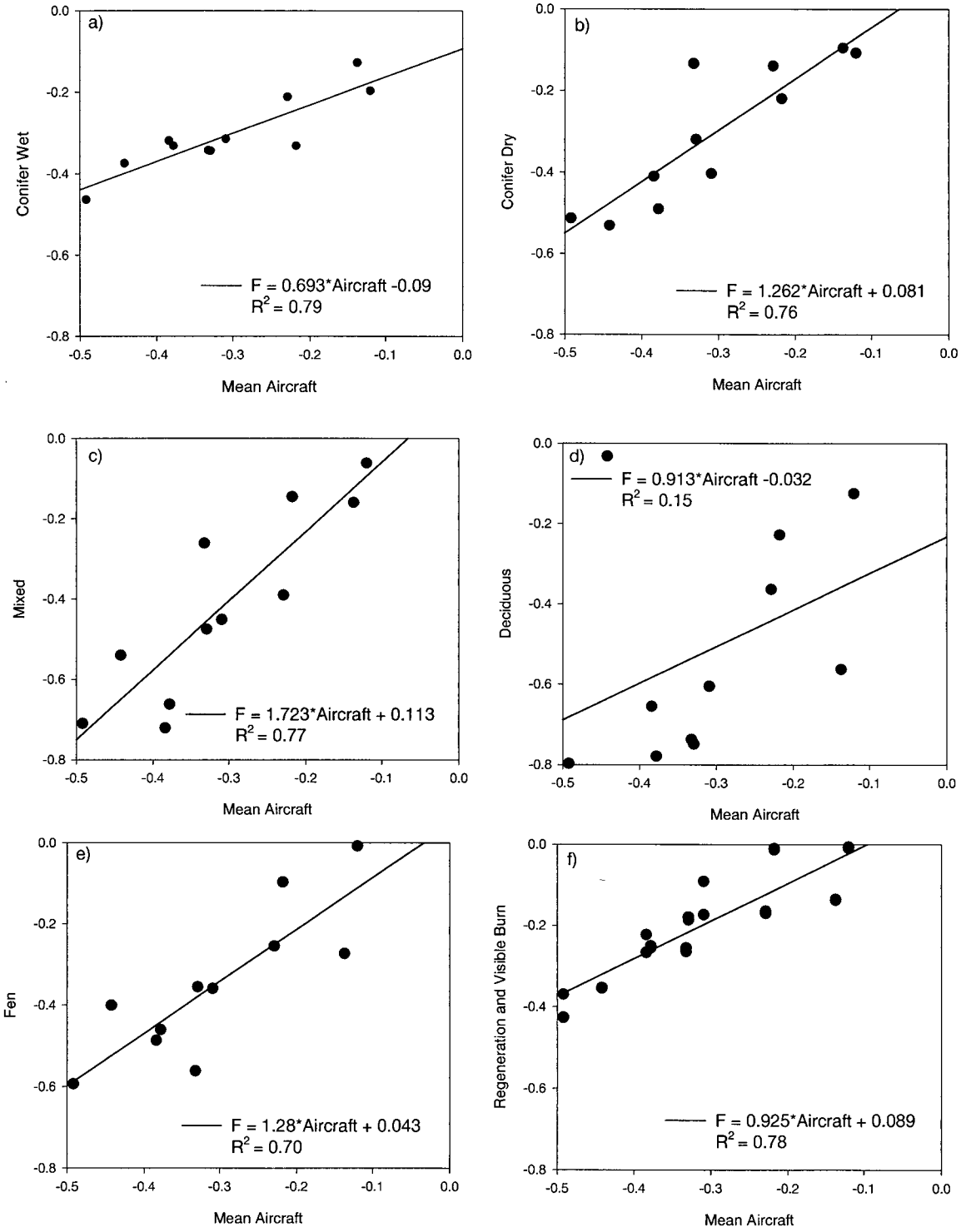

Figure 14. Linear relationship between the mean aircraft CO_2 flux (mg m^{-2} s^{-1}) in 1994 and 1996 and the unmixed flux obtained using CW and De forcings for the main cover types: (a) conifer wet, (b) conifer dry, (c) mixed, (d) deciduous, (e) fen, and (f) regeneration and visible burn.

close to zero. However, under the CW and De constraints, large departures from the zero intercept are found: CW and De both have a sizable negative intercept while the others have a positive intercept. Ecologically, the positive intercept for Re and VB is reasonable because in these cover types, soil respiration can exceed net photosynthesis during the day. However, for Mi it is unreasonable to see the positive intercept while CW and De have negative intercepts. It may also be unreasonable for the positive intercepts for CD and Fe. These unreasonable changes in intercept are caused by the CW constraint using the OBS tower measurements. It seems that the downward flux measured at the OBS tower was generally larger than the corresponding aircraft value derived under the CLLS constraint. The relative difference was the largest when the flux

was the smallest, causing the changes in the slope and intercept under the CW constraint. These changes in this dominant cover type are then compensated by changes in other cover types in the opposite direction. The tight tower constraint approach can therefore lead to unreasonable shares of the aircraft-measured flux among the different cover types when the tower measurements are not representative. The R^2 value can be used to help judge whether the tower constraint has improved upscaling under the assumption that the proportions of the various cover types in the landscape in the total measured flux are not changing with time, i.e., are the same on the different days of flight. We indeed found that under the tower constraints the R^2 value improves from the CLLS case for Mi, Fe, Re, and VB, indicating some positive impacts of the tower constraints (mostly the CW constraint in this case). The R^2 value decreases for CW because of the decrease in slope. The OA forcing for the De type overcomes the problem of underestimating the De flux using the CLLS method because of the small area fraction and the usually large De downward flux compared with that of the adjacent cover types, but the scatter of data points for De increases under the OA forcing. This increase indicates either that the OA tower measurements were not always representative of the same cover type within the flight grid or that it is difficult to determine the actual value from aircraft because of the small area fraction. From the above analysis we conclude that tower measurements can generally improve the unmixing results, but precautions should be taken to prevent excessive tower constraining from causing biases for all other cover types. A quantitative method is yet to be developed to base the strength of constraint on the representativeness of tower measurements. We can also infer that in other areas, where the internal differences within cover types are smaller than the differences between cover types and all cover types have significant area fractions, the flux unmixing can be made without ground assistance.

The second question can also be addressed using Figures 13 and 14. Because of the good relationship between the aircraft mean and the flux from the dominant cover type CW, the aircraft mean flux can be replaced by the CW flux without significantly altering the relationships shown in Figures 13 and 14. This means that if tower measurements in the dominant cover type are available for other times and days, these aircraft-based relationships can be used to scale the tower measurements to the region surrounding the tower. The underlying assumptions for such a simple scaling method are as follows: (1) The whole region undergoes the same weather conditions (radiation, temperature, rainfall, etc.) in such a way that the fluxes to the various cover types are highly correlated, and (2) the physiological differences between the various cover types are already taken into account in the slope of the aircraft-based relationships (for example, De has a larger slope than Re and VB). It is obvious that these assumptions do not always hold, especially immediately after rainfalls when the soil water balance is strongly dependent on soil texture and will unevenly affect CO_2 uptake across the landscape. Nevertheless, the use of aircraft in this way to fill in data gaps for other cover types should generally improve from regional estimations solely based on limited tower measurements.

Further research is required to determine the feasibility of obtaining daily regional CO_2 fluxes using the combination of discrete aircraft measurements and continuous tower measurements. Temporal scaling of CO_2 fluxes is complicated by the diurnal patterns of meteorological variables affecting both daytime photosynthesis and respiration and nighttime respiration. The same aircraft flux-unmixing methodology may be adopted for obtaining instantaneous and daily H_2O fluxes for large areas.

5. Summary

We have demonstrated that it is feasible to separate the aircraft flux measurements into fluxes for the major cover types in the underlying surface using a linear unmixing method. The use of a footprint function, to consider the effect of atmospheric dispersion from surfaces at different upwind distances, and the use of mathematical constraints, to suppress the influence of various sampling errors or to include independent ground (tower) measurements in the analysis, are the two critical components of the unmixing method. The unmixing method produces reasonable results for all cover types with significant area fractions (>5%). The use of simultaneous tower flux measurements as part of the mathematical constraint generally improves the unmixing results, but the improvement strongly depends on the representativeness of the tower measurements. A mathematical scheme is yet to be developed to determine the degree of the constraint based on the representativeness.

Aircraft-based flux measurements help regional estimation of CO_2 flux by providing large area averaged fluxes for individual cover types in the region. When tower-based measurements are available for a few cover types, the aircraft technique is a useful means to scale up from tower to region for the following two main reasons: (1) It provides estimates for all cover types that are significant in the region, and (2) it has the potential of quantifying the representativeness of individual tower measurements. Such an aircraft-tower combined approach has the potential to reduce the number of flux towers usually required in large-scale experiments such as BOREAS.

Strong correlations exist between aircraft mean flux measurements and the fluxes from the individual cover types, suggesting that environmental conditions generally had similar effects on vegetation growth for the various cover types in the same region. These strong correlations explain why it is possible to produce first-order regional estimates of CO_2 flux using aircraft measurements for the region and tower measurements in a few cover types.

Acknowledgments. We thank Jinhui Huang and Qinghan Xiao for assistance in developing programs for footprint calculations and automatic image extractions. Funding for the Twin Otter operations in BOREAS was provided by the Natural Sciences and Engineering Research Council (to Peter Schuepp of McGill University), Agriculture and Agri-Food Canada, the Atmospheric Environment Service, and the National Research Council of Canada. The tower flux measurements were made by E. Pattey of Agriculture and Agri-Food Canada, A. T. Black of the University of British Columbia, D. Baldocchi of Oak Ridge National Laboratory of NOAA, Dean Anderson of the U.S. Geological Survey, and S. Verma of the University of Nebraska. The manuscript was internally reviewed by W. Chen before submission.

References

Black, T. A., et al., Annual cycle of water vapour and carbon dioxide fluxes in and above a boreal aspen forest, *Global Change Biol.*, *2*, 101–111, 1997.

Desjardins, R. L., Airborne test of flux measurements by the relaxed eddy accumulation technique, *Monograph on Advances in Bioclimatology*, edited by G. Stanhill, pp. 1–41, Springer-Verlag, New York, 1991.

Desjardins, R. L., P. H. Schuepp, J. I. MacPherson, and D. J. Buckley,

Spatial and temporal variation of the fluxes of carbon dioxide and sensible and latent heat over the FIFE site, *J. Geophys. Res*., *97*, 18,467–18,476, 1992.

Desjardins, R. L., J. I. MacPherson, P. H. Schuepp, and H. Hayhoe, Airborne flux measurements of CO_2 and H_2O over the Hudson Bay Lowlands, *J. Geophys. Res*., *99*, 1551–1561, 1994.

Desjardins, R. L., J. I. MacPherson, H. Neuman, G. den Hartog, and P. H. Schuepp, Flux estimate of latent and sensible heat, carbon dioxide and ozone using aircraft-tower combination, *Atmos. Environ*., *29*, 3147–3158, 1995.

Desjardins, R. L., et al., Scaling up-flux measurements for the boreal forest using aircraft-tower combination, *J. Geophys. Res*., *102*, 29,125–29,134, 1997.

Goulden, M. L., B. C. Daube, S. M. Fan, D. J. Sutton, A. Bazzaz, J. W. Munger, S. C. Wofsy, P. M. Crill, J. W. Harden, and S. E. Trumbore, Sensitivity of boreal forest carbon balance to soil thaw, *Science*, *279*, 214–217, 1998.

Grace, J., et al., Carbon dioxide uptake by an undisturbed tropical rain forest in Southwest Amazonia, 1992 to 1993, *Science*, *270*, 778–780, 1995.

Hall, F. G., D. E. Knapp, and K. F. Huemmrich, Physically based classification and satellite mapping of biophysical characteristics in the southern boreal forest, *J. Geophys. Res*., *102*, 29,567–29,580, 1997.

Horst, T. W., and J. C. Weil, Footprint estimation for scalar flux measurements in the atmospheric surface layer, *Boundary Layer Meteorol*., *59*, 279–296, 1992.

Horst, T. W., and J. C. Weil, How far is far enough?: The fetch requirements for micrometeorological measurements of surface fluxes, *J. Atmos. Oceanic Technol*., *11*, 1018–1025, 1994.

Kaharabata, S. K., P. H. Schuepp, S. Ogunjemiyo, S. Shen, M. Y. Leclerc, R. L. Desjardins, and J. I. Macpherson, Footprint consideration in BOREAS, *J. Geophys. Res*., *102*, 29,113–29,124, 1997.

MacPherson, J. I., NRC Twin Otter operations in BOREAS 1994, *Rep. LTR-FR-129*, Natl. Res. Counc. of Can., Ottawa, 1996.

MacPherson, J. I., and M. Bastian, NRC Twin Otter operations in BOREAS 1996, *Rep. LTR-FR-134*, Natl. Res. Counc. of Can., Ottawa, 1997.

MacPherson, J. I., and A. K. Betts, Aircraft encounters with strong coherent vortices over boreal forest, *J. Geophys. Res*., *102*, 29,231–29,234, 1997.

Mahrt, L., Flux sampling errors for aircraft and tower, *J. Atmos. Oceanic Technol*., *15*, 416–429, 1998.

Mitic, C. M., P. H. Schuepp, R. L. Desjardins, and J. I. MacPherson, Spatial distribution and co-occurrence of surface-atmosphere energy and gas exchange processes over the code grid site, *Atmos. Environ*., *29*, 3169–3180, 1995.

Ogunjemiyo, S., P. H. Schuepp, J. I. MacPherson, and R. L. Desjardins, Analysis of flux maps versus surface characteristics from Twin Otter grid flights in BOREAS 1994, *J. Geophys. Res*., *102*, 29,135–29,145, 1997.

Perry, S. G., A. B. Fraser, D. W. Thomson, and J. M. Norman, Indirect sensing of plant canopy structure with simple radiation measurements, *Agric. For. Meteorol*., *42*, 255–278, 1988.

Schmid, H. P., and T. R. Oke, A model to estimate the source area contributing to turbulent exchange in the surface layer over patchy terrain, *Q. J. R. Meteorol. Soc*., *116*, 956–988, 1990.

Schuepp, P. H., M. Y. Leclerc, J. I. MacPherson, and R. L. Desjardins, Footprint prediction of scalar fluxes from analytical solutions of the diffusion equation, *Boundary Layer Meteorol*., *50*, 355–373, 1990.

Schuepp, P. H., J. I. MacPherson, and R. L. Desjardins, Adjustment of footprint correction for airborne flux mapping over the FIFE site, *J. Geophys. Res*., *97*, 18,455–18,466, 1992.

Stull, R. B., *An Introduction to Boundary Layer Meteorology*, 666 pp., Kluwer Acad., Norwell, Mass., 1988.

Twomey, S., *Developments in Geomathematics 3: Introduction to the Mathematics of Inversion in Remote Sensing and Indirect Measurements*, 243 pp., Elsevier Sci., New York, 1977.

J. M. Chen, J. Cihlar, and S. G. Leblanc, Canada Centre for Remote Sensing, 588 Booth Street, 4th Floor, Ottawa, Ontario, Canada K1A 0Y7. (jing.chen@ccrs.nrcan.gc.ca; josef.cihlar@geocan.nrcan.gc.ca)

R. L. Desjardins, Agriculture and Agri-Food Canada, Central Experimental Farm, Building 74, Ottawa, Ontario, Canada K1A 0C6. (desjardins@em.agr.ca)

J. I. MacPherson, Flight Research Laboratory, National Research Council of Canada, Building U61, Ottawa, Ontario, Canada K1A 0R6. (ian.macpherson@nrc.ca)

(Received July 12, 1998; revised February 18, 1999;
accepted February 23, 1999.)